

# The minimum and maximum gravitational-wave background from supermassive binary black holes

Xing-Jiang Zhu<sup>1,2\*</sup>, Weiguang Cui<sup>3</sup> and Eric Thrane<sup>1,2</sup>

<sup>1</sup>*School of Physics and Astronomy, Monash University, Clayton, Vic 3800, Australia*

<sup>2</sup>*OzGrav: The Australian Research Council Centre of Excellence for Gravitational Wave Discovery*

<sup>3</sup>*Departamento de Física Teórica, Módulo 15, Facultad de Ciencias, Universidad Autónoma de Madrid, 28049 Madrid, Spain*

Accepted XXX. Received YYY; in original form ZZZ

## ABSTRACT

The gravitational-wave background from supermassive binary black holes (SMBBHs) has yet to be detected. This has led to speculations as to whether current pulsar timing array limits are in tension with theoretical predictions. In this paper, we use electromagnetic observations to constrain the SMBBH background from above and below. To derive the *maximum* amplitude of the background, we suppose that equal-mass SMBBH mergers fully account for the local black hole number density. This yields a maximum characteristic signal amplitude at a period of one year  $A_{\text{yr}} < 2.4 \times 10^{-15}$ , which is comparable to the pulsar timing limits. To derive the *minimum* amplitude requires an electromagnetic observation of an SMBBH. While a number of candidates have been put forward, there are no universally-accepted electromagnetic detections in the nanohertz band. We show the candidate 3C 66B implies a lower limit, which is inconsistent with limits from pulsar timing, casting doubt on its binary nature. Alternatively, if the parameters of OJ 287 are known accurately, then  $A_{\text{yr}} > 6.1 \times 10^{-17}$  at 95% confidence level. If one of the current candidates can be established as a bona fide SMBBH, it will immediately imply an astrophysically interesting lower limit.

**Key words:** gravitational waves – galaxies: evolution – quasars: individual(OJ 287) – galaxies: individual(3C 66B) – black hole physics – pulsars: general

## 1 INTRODUCTION

The detection of gravitational waves (GWs) from several stellar-mass compact binary merger events (Abbott et al. 2016a, 2017a,b) by ground-based laser interferometers Advanced LIGO (Aasi et al. 2015) and Advanced Virgo (Acernese et al. 2015) heralded a new era of GW astronomy. In parallel to ground-based detectors that are monitoring the audio band ( $\sim 10 - 10^3$  Hz) of the GW spectrum, decades of efforts have gone into opening the nanohertz frequency ( $10^{-9} - 10^{-7}$  Hz) window (Sazhin 1978; Detweiler 1979; Hellings & Downs 1983; Jenet et al. 2005; Hobbs et al. 2010; Manchester 2013). These experiments, called pulsar timing arrays (PTAs; Foster & Backer 1990), use a number of ultra stable millisecond pulsars collectively as a Galactic-scale GW detector.

Previous PTA searches (e.g., Yardley et al. 2011; van Haasteren et al. 2011; Demorest et al. 2013) have primarily targeted a GW background (GWB) formed by a cosmic population of supermassive binary black holes (SMBBHs;

Begelman et al. 1980). Assuming that binaries are circular with the orbital evolution driven by GW emission, the characteristic amplitude  $h_c$  of such a background signal can be well described by a power-law spectrum  $h_c \sim f^{-2/3}$  with  $f$  being GW frequency (Phinney 2001); the amplitude at  $f = 1 \text{ yr}^{-1}$ , denoted by  $A_{\text{yr}}$ , can be conveniently used for comparing steadily-improving experimental limits and different model predictions. Prior to the formation of timing arrays, Kaspi et al. (1994) used long-term observations of two pulsars to constrain  $A_{\text{yr}} \leq 2.6 \times 10^{-14}$  with 95% confidence (the same confidence level applied for limits quoted below). Jenet et al. (2006) reduced this limit to  $1.1 \times 10^{-14}$  using a prototype data set of the Parkes Pulsar Timing Array (PPTA; Manchester et al. 2013). Since the establishment of three major PTAs, including PPTA, NANOGrav (McLaughlin 2013) and the European PTA (EPTA; Kramer & Champion 2013), the constraints have been improved by an order of magnitude over the last decade. Currently the best published upper limit on  $A_{\text{yr}}$  is  $1 \times 10^{-15}$  by the PPTA (Shannon et al. 2015) with comparable results from the other two PTAs (Lentati et al. 2015; Arzoumanian et al. 2018). The three PTAs have joined together to form the Interna-

\* E-mail: xingjiang.zhu@monash.edu

tional Pulsar Timing Array (IPTA; Verbiest et al. 2016), aiming at a more sensitive data set.

Over the past two decades, theoretical predictions of  $A_{\text{yr}}$  have also evolved. Rajagopal & Romani (1995) considered several mechanisms that can drive SMBBHs into the GW emission regime and obtained an estimate of  $A_{\text{yr}} = 2.2 \times 10^{-16}$ . Jaffe & Backer (2003) used galaxy merger rate estimates and the scaling relation between black hole mass and the spheroid mass of its host galaxy to compute the GWB spectrum; they confirmed the power-law relation and found  $A_{\text{yr}} \sim 10^{-15}$ . Subsequently, Wyithe & Loeb (2003) employed a comprehensive set of semi-analytical models of dark matter halo mergers and the scaling relation between black hole mass and the velocity dispersion of its host galaxy; they found that the GWB is dominated by sources at redshifts  $z \lesssim 2$ . Most of recent studies generated consistent results with median values at  $A_{\text{yr}} \approx 1 \times 10^{-15}$  (Sesana et al. 2008; Sesana 2013; Ravi et al. 2014), whereas some suggested that the signal may be a factor of two stronger (Kulier et al. 2015) or even a factor of four stronger (McWilliams et al. 2014).

Theoretical prediction of the GWB is essential to the interpretation of current PTA upper limits. In Shannon et al. (2015), theoretical models that predict typical signals of  $A_{\text{yr}} \gtrsim 1 \times 10^{-15}$  were ruled out with high ( $\gtrsim 90\%$ ) confidence. It was further suggested that the orbital evolution of SMBBHs is either too fast (e.g., accelerated by interaction with ambient stars and/or gas) or stalled. Such a tension between models and observations can be eliminated using different black hole-host scaling relations (Sesana et al. 2016). Recently, Middleton et al. (2018) quantified this problem within a Bayesian framework by comparing a wide range of models with the PPTA limit and found that only the most optimistic scenarios are disfavoured.

Furthermore, understanding uncertainties in  $A_{\text{yr}}$  predictions is critical to the evaluation of future detection prospects. For example, in Taylor et al. (2016), the model of Sesana (2013) was used in combination with PTA upper limits to calculate the time to detection of the GWB. Based on simple statistical estimates, they suggested  $\sim 80\%$  of detection probability within the next ten years for a large and expanding timing array. Needless to say, this statement hinges on accurate predictions of the minimum GWB. Dvorkin & Barausse (2017) attempted to make such a prediction within a semi-analytical galaxy formation model by artificially stalling all SMBBHs at the orbital separation from which GW can drive binaries to merge within a Hubble time; they suggested that a PTA based on the Square Kilometre Array (SKA; Lazio 2013) is capable of making a detection in this least favourable scenario. Recently, Bonetti et al. (2018) and Ryu et al. (2018) showed that this scenario might be too pessimistic because triple/multiple interactions can drive a considerable fraction of stalling binaries to merge; both suggested that the GWB is unlikely to be lower than  $A_{\text{yr}} \sim 10^{-16}$ .

In this paper, we first assess the implication of current PTA upper limits. We approach this issue differently from previous studies. We point out that the local black hole mass function, an electromagnetically determined measure of the number density of black holes as a function of mass, implies a constraint on  $A_{\text{yr}}$ . If we suppose all black holes are produced by equal-mass SMBBH mergers, then the black hole mass function gives us a maximum GWB amplitude.

Second, we present a novel Bayesian framework to infer the SMBBH merger rate based on a gold-plated detection of a single system. The derived merger rate can be combined with the system chirp mass to compute the GWB signal amplitude using the practical theorem of Phinney (2001). We consider several SMBBH candidates with inferred masses and orbital periods, and derive lower bounds on  $A_{\text{yr}}$ .

This paper is organized as follows. In Section 2, we review the formalism of Phinney (2001) and provide two useful equations for quick computation of  $A_{\text{yr}}$ . In Section 3, we derive the maximum signal amplitude from several black hole mass functions. In Section 4 we present the Bayesian framework for inferring the SMBBH merger rate from a single system. We apply this method to several SMBBH candidates to derive plausible lower bounds of  $A_{\text{yr}}$ . Finally, Section 5 contains summary and discussions.

## 2 THE FORMALISM

In this section we present a phenomenological model for the GWB formed by a population of SMBBHs in circular orbits. We start from the calculation of  $\Omega_{\text{GW}}(f)$  – the GW energy density per logarithmic frequency interval at observed frequency  $f$ , divided by the critical energy density required to close the Universe today  $\rho_c = 3H_0^2 c^2 / 8\pi G$ . Here  $H_0$  is the Hubble constant. Assuming a homogeneous and isotropic Universe, it is straightforward to compute this dimensionless function as (see Phinney 2001, for details):

$$\Omega_{\text{GW}}(f) = \frac{1}{\rho_c} \int_0^\infty \frac{N(z)}{(1+z)} \left( \frac{dE_{\text{GW}}}{d \ln f_r} \right) \Big|_{f_r=f(1+z)} dz, \quad (1)$$

where  $N(z)$  is the spatial number density of GW events at redshift  $z$ ; the  $(1+z)$  factor accounts for the redshifting of GW energy;  $f_r = f(1+z)$  is the GW frequency in the source's cosmic rest frame, and  $d f_r (dE_{\text{GW}}/d f_r)$  is the total energy emitted in GWs within the frequency interval from  $f_r$  to  $f_r + d f_r$ .

There are two other quantities that are commonly used for the characterization of a GWB, namely, the one-sided spectral density  $S_h(f)$  and the characteristic amplitude  $h_c(f)$ . They are related to  $\Omega_{\text{GW}}(f)$  by (Maggiore 2000):

$$h_c^2(f) = f S_h(f) = \frac{3H_0^2}{2\pi^2} f^{-2} \Omega_{\text{GW}}(f). \quad (2)$$

In the Newtonian limit, the GW energy spectrum for an inspiralling circular binary of component masses  $m_1$  and  $m_2$  is given by (Thorne 1987):

$$\frac{dE_{\text{GW}}}{df} = \frac{(\pi G)^{2/3} M_c^{5/3}}{3} f^{-1/3}, \quad (3)$$

where  $M_c$  is the chirp mass defined as  $M_c = M\eta^{3/5}$ , with  $M = m_1 + m_2$  being the total mass and  $\eta = m_1 m_2 / M^2$  being the symmetric mass ratio. Equation (3) is a good approximation up to the frequency at the last stable orbit during inspiral  $f_{\text{max}} \approx 4.4 \text{ kHz} / (M/M_\odot)$ . The merger and ringdown processes occur beyond the PTA band and thus their contribution to the GWB is ignored (Zhu et al. 2011).

For SMBBHs, if we assume that 1) the binary can reach a separation of  $\sim 1 \text{ pc}$  so that dynamical friction becomes ineffective; and 2) the binary hardens through the repeated scattering of stars in the core of the host, then there exists

a minimum frequency  $f_{\min}$  for equation (3) to be valid as given by (Quinlan 1996):

$$f_{\min} = 2.7 \text{ nHz} \left[ \frac{m_1 m_2}{(10^8 M_\odot)^2} \right]^{-0.3} \left( \frac{m_1 + m_2}{2 \times 10^8 M_\odot} \right)^{0.2}. \quad (4)$$

The characteristic amplitude of the GWB formed by a cosmological population of SMBBHs in circular orbits is given by:

$$h_c^2(f) = \frac{4G^{5/3}}{3c^2\pi^{1/3}f^{4/3}} \int \int \frac{d^2N}{dM_c dz} M_c^{5/3} (1+z)^{-1/3} dM_c dz, \quad (5)$$

where  $\frac{d^2N}{dM_c dz}$  is the number density (per unit comoving volume) of SMBBH mergers within chirp mass range between  $M_c$  and  $M_c + dM_c$ , and a redshift range between  $z$  and  $z + dz$ . The integration is typically performed over  $10^7 - 10^{10} M_\odot$  for  $M_c$  and  $0 - 2$  for  $z$  (see, e.g., Sesana 2013). In this work, we assume that the binary orbital evolution above  $f_{\min}$  is driven solely by GWs. This leads to a  $h_c \sim f^{-2/3}$  relation for the frequency band ( $1 \text{ nHz} \lesssim f \lesssim 100 \text{ nHz}$ ) of interest to PTAs (Sesana 2013; Ravi et al. 2014; McWilliams et al. 2014).

To compute  $h_c(f)$ , one needs to know the distribution of SMBBHs in chirp mass and redshift. Previous studies relied on galaxy merger rate as a function of redshift, which are typically derived from cosmological simulations of galaxy formation or observations of galaxy pair fraction combined with galaxy merger timescale, and various black hole-host galaxy scaling relations. In this work, we take a different approach. First of all, we note that equation (5) can be simplified by assuming that there is no redshift dependency for black hole mass distribution. While this is incorrect, we show in the next sections that its effect is small.

Below we provide two useful equations for computing  $h_c$  in convenient numerical forms. The first is adapted from Zhu et al. (2013) and states

$$h_c(f) = 4.8 \times 10^{-16} \left( \frac{10^4 \times r_0}{\text{Mpc}^{-3} \text{Gyr}^{-1}} \right)^{1/2} \left[ \frac{\langle M_c^{5/3} \rangle}{(10^8 M_\odot)^{5/3}} \right]^{1/2} \times \left( \frac{I_{-4/3}}{0.63} \right)^{1/2} \left( \frac{f}{1 \text{ yr}^{-1}} \right)^{-2/3}, \quad (6)$$

where  $r_0$  is the local SMBBH merger rate density. A second form is adapted from Phinney (2001)

$$h_c(f) = 1.5 \times 10^{-16} \left( \frac{10^4 \times N_0}{\text{Mpc}^{-3}} \right)^{1/2} \left[ \frac{\langle M_c^{5/3} \rangle}{(10^8 M_\odot)^{5/3}} \right]^{1/2} \times \left( \frac{I_{-4/3}}{0.86 I_{-1}} \right)^{1/2} \left( \frac{f}{1 \text{ yr}^{-1}} \right)^{-2/3}. \quad (7)$$

where  $N_0$  is the present-day comoving number density of SMBBH merger remnants. In both equations above,  $\langle M_c^{5/3} \rangle$  represents the average contribution of coalescing binaries to the energy density of the GWB, and we have defined the following quantity (e.g., Zhu et al. 2013)

$$I_\alpha = \int_{z_{\min}}^{z_{\max}} \frac{e(z)(1+z)^\alpha}{\sqrt{\Omega_\Lambda + \Omega_m(1+z)^3}} dz. \quad (8)$$

Here  $z_{\min} = \max(0, f_{\min}/f - 1)$  and  $z_{\max} = \min(z_\star, f_{\max}/f - 1)$  with  $z_\star$  representing the beginning of source formation, and  $e(z)$  is a dimensionless function that accounts for the cosmic evolution of merger rate density. We set  $z_{\min} = 0$

and  $z_{\max} = 2$  since sources in this redshift range make the majority contribution to the GWB. Throughout this paper, we assume a standard  $\Lambda$ CDM cosmology with parameters  $H_0 = 67.8 \text{ km s}^{-1} \text{ Mpc}^{-1}$ ,  $\Omega_m = 0.308$  and  $\Omega_\Lambda = 0.692$  (Planck Collaboration et al. 2016).

In Equations (6-7),  $I_{-4/3} = 0.63$  and  $I_{-4/3}/I_{-1} = 0.86$  are used as fiducial values in the case of  $e(z) = 1$ , i.e., the merger rate remains constant between  $z = 0$  and  $z = 2$ . Both factors are insensitive to details of  $e(z)$ . For example, assuming  $e(z) = (1+z)^m$ ,  $(I_{-4/3}/0.63)^{1/2}$  only increases from 0.83 for  $m = -1$  to 1.26 for  $m = 1$ , whereas the change in  $(I_{-4/3}/0.86 I_{-1})^{1/2}$  is even smaller – only varying from 1.01 for  $m = -1$  to 0.99 for  $m = 1$ .

The focus of this paper is to the maximum and minimum GWB signal amplitudes, represented by  $A_{\text{yr}}$  for the power-law model

$$h_c(f) = A_{\text{yr}} \left( \frac{f}{1 \text{ yr}^{-1}} \right)^{-2/3}. \quad (9)$$

### 3 THE MAXIMUM SIGNAL

The black hole mass function defines the number density of black holes as a function of mass. Assuming that all the black holes were produced by equal-mass binary mergers and that mass function does not evolve across cosmic time<sup>1</sup>, the double integral in Equation (5) can be factorized, leading to the following quantity which defines the maximum signal amplitude allowed by the local black hole mass function

$$(A_{\text{yr}}^{\max})^2 = \frac{4G^{5/3}\eta_{\max}}{3c^2\pi^{1/3}f_{\text{yr}}^{4/3}} \int \frac{dN}{dM} (1.1M)^{5/3} dM \int_0^2 (1+z)^{-1/3} dz, \quad (10)$$

where  $f_{\text{yr}} = \text{yr}^{-1} \simeq 3.17 \times 10^{-8} \text{ Hz}$ ,  $\eta_{\max} = 0.25$  is the maximum value of  $\eta$  when  $m_1 = m_2$ ,  $dN/dM$  is the black hole mass function at  $z = 0$ . In Equation (10)  $M$  denotes masses of the final black holes produced by SMBBH mergers. We assume 10% of rest-mass energy is radiated away in GWs during the inspiral-merger-ringdown process<sup>2</sup>, the binary total mass is  $1.1M$ , which determines the GW emission during inspirals.

Here we consider a range of mass functions determined with different black hole-host scaling relations (Marconi et al. 2004; Li et al. 2011; Shankar 2013; Ueda et al. 2014; Mutlu-Pakdil et al. 2016). We provide details of these models in Appendix A and summarize our results here. In Figure 1, we plot the probability distribution of  $A_{\text{yr}}^{\max}$ , where the spread is directly translated from measurement uncertainties in black hole mass functions (shown in Figure A1) through Monte-Carlo simulations.

Among the mass functions considered, the model by Shankar (2013) yields the highest median  $A_{\text{yr}}^{\max}$  at  $1.8 \times 10^{-15}$ . While the maximum possible GWB *could* be this high, there are good reasons to expect it to be lower. First, a uniform distribution of mass ratio ( $q = m_2/m_1$ ) between 0 and 1

<sup>1</sup> The mass function must evolve if all black holes are made from equal-mass mergers. We enforce such an assumption since we are only concerned with the maximum signal.

<sup>2</sup> Such a radiation efficiency can be seen as an upper bound (Flanagan & Hughes 1998).

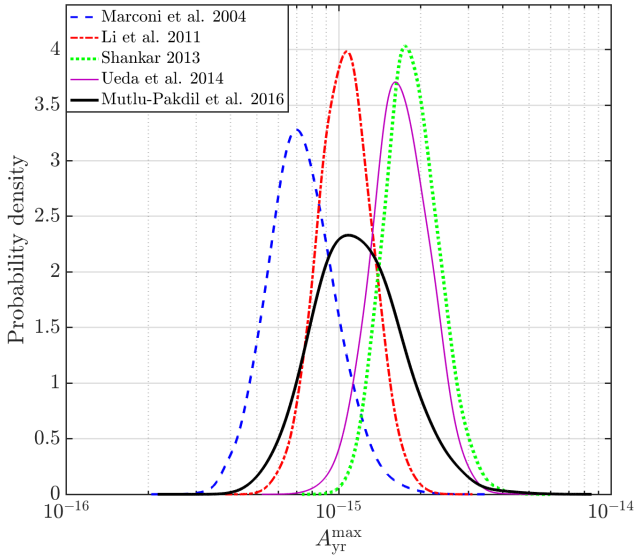


**Figure 1.** Probability distribution of  $A_{\text{yr}}^{\text{max}}$  derived from a range of local black hole mass functions (see text for details).

gives an average  $\langle \eta \rangle = 0.193$ . This corresponds to a factor of  $\sqrt{\eta_{\text{max}}/\langle \eta \rangle} = 1.14$ . Second, a more realistic radiation efficiency is 5%, resulting in a factor of  $(1.1/1.05)^{5/6} = 1.04$ . Third, we make use of the black hole mass function at higher redshifts to compute the following quantity:

$$A_z = \left( \frac{\int_{M_{\text{min}}}^{M_{\text{max}}} \frac{dN}{dM} (z=0) M^{5/3} dM \int_0^2 (1+z)^{-1/3} dz}{\int_{M_{\text{min}}}^{M_{\text{max}}} \int_0^2 \frac{d^2 N}{dM dz} M^{5/3} (1+z)^{-1/3} dM dz} \right)^{1/2}. \quad (11)$$

Using the data presented in Ueda et al. (2014), we find  $A_z = 1.1$  for  $M_{\text{min}} = 10^7 M_{\odot}$  and  $M_{\text{max}} = 10^{10} M_{\odot}$ . Overall, a more realistic estimate would be multiplying  $A_{\text{yr}}^{\text{max}}$  as given by Equation (10) and illustrated in Figure 1 by  $\frac{1}{1.14 \times 1.04 \times 1.10} = 0.77$ .

To demonstrate the effectiveness of our calculations, we take the black hole mass function used in Sesana (2013) (illustrated as solid black lines in the upper panel of their fig. 1), compute  $A_{\text{yr}}^{\text{max}}$  and then multiply by 0.77. This gives  $5.0 \times 10^{-16} < A_{\text{yr}} < 1.1 \times 10^{-15}$  with 68% confidence. This matches well with the interval of  $3.8 \times 10^{-16} < A_{\text{yr}} < 1.1 \times 10^{-15}$  at the same confidence level for their fiducial model.

#### 4 THE MINIMUM SIGNAL

Suppose that there is a gold-plated detection of SMBBH system with measured chirp mass, orbital period and distance. We show here that it can be used to derive a lower limit on the GWB. A similar approach has been taken to estimate contributions from stellar-mass binary mergers to a GWB signal in the ground-based detector band. For example, the first binary black hole merger GW150914 (Abbott et al. 2016b) and the first binary neutron star inspiral GW170817 (Abbott et al. 2017a) were both used to infer the corresponding GWB level, for which the uncertainty is dominated by Poissonian errors of the merger rate (Abbott et al. 2016c, 2018).

Here we begin with the description of our framework for performing Bayesian inference on the SMBBH merger rate, and then apply it to several well-established SMBBH candidates. First, a naive estimator ( $\hat{r}_0$ ) for the merger rate density  $r_0$  associated with a single SMBBH is

$$\hat{r}_0 = \frac{1}{\epsilon V_0 T_c}, \quad (12)$$

where  $\epsilon$ , taking values between 0 and 1, is the detection efficiency whose definition is discussed in detail below;  $V_0$  is the comoving volume at the source (comoving) distance  $d$ , which is given by  $(4\pi/3)d^3$ ;  $T_c$  is the binary coalescence time as a result of gravitational radiation. For a circular binary,  $T_c$  is given by (Thorne 1987)

$$T_c = \frac{5c^5}{256(2\pi f_0)^{8/3}(GM_c)^{5/3}}, \quad (13)$$

where  $f_0 = 1/P_b$  is the observed binary orbital frequency with  $P_b$  being the orbital period. For a binary with measured eccentricity  $e_0$ , the coalescence time can be well approximated by multiplying the above equation by  $\exp(-4e_0^2)$  if  $e_0 \lesssim 0.7$ .

The electromagnetic detection of an SMBBH will encode two pieces of information: that there is at least  $N = 1$  SMBBH and that it was observed at a (co-moving) distance of  $\hat{d}$ . The true distance is  $d$  (no hat). The detection efficiency  $\epsilon$  in Equation (12) is used to account for two factors. First, it accounts for the incompleteness of the survey that discovered the SMBBH system. For example, the search may have only covered part of the sky. Second, it accounts for the fact that nearby binaries could be missed even if they are in the sky region included in the survey. For example, if there are two binaries with identical component masses, distances, and orbital period, but with different viewing angles, one may be detectable while the other is not (see, e.g., the scenario discussed in D’Orazio et al. 2015). For the purpose of estimating the minimum signal, we assume  $\epsilon = 1$ , which underestimates the merger rate.

In reality, many SMBBH candidates, such as those considered in our study, have been discovered serendipitously; they were not discovered via a systematic survey. However, we can model these serendipitous discoveries by parameterizing the unknown detection efficiency. We parameterize this efficiency curve as a step function, which is unity for  $d < d_{\text{max}}$  and zero for  $d > d_{\text{max}}$ . This is a reasonable approximation given the rate at which distant objects become dimmer with distance. Having made this assumption, we use the data itself to infer  $d_{\text{max}}$ . The physical interpretation of  $d_{\text{max}}$  is that it is the “effective maximum detection distance” for whatever measurements led to the discovery of an SMBBH candidate. We model the likelihood of the observation of an SMBBH as  $\mathcal{L}(N, \hat{d}|d, r_0, d_{\text{max}})$  where  $N = 1$  is the number of observed SMBBH in some observable volume. The likelihood is a Poisson distribution

$$\mathcal{L}(N, \hat{d}|d, r_0, d_{\text{max}}; \epsilon = 1) = \lambda e^{-\lambda} \delta(d - \hat{d}) \quad (14)$$

where  $\lambda$ , the average number of SMBBH,

$$\lambda = r_0 V T_c \quad (15)$$

$$= r_0 \left( \frac{4}{3} \pi d_{\text{max}}^3 \right) T_c, \quad (16)$$

depends on the rate  $r_0$ , the visible volume  $V = (4\pi/3)d_{\text{max}}^3$ ,

and the binary coalescence time  $T_c$ . By introducing a delta function  $\delta(d - \hat{d})$ , we assume that the distance is measured with high precision.

Assuming that sources are uniformly distributed in co-moving volume up to  $d_{\max}$ , the conditional probability of observing one source at distance  $d$  is given by

$$\pi(d|d_{\max}) = \frac{3d^2}{d_{\max}^3} \Theta(d_{\max} - d), \quad (17)$$

where  $\Theta$  is the Heaviside step function:  $\Theta(x) = 1$  for  $x \geq 0$  and  $\Theta(x) = 0$  otherwise. Applying Bayes' theorem, we obtain a posterior distribution for the rate  $r_0$  and the maximum distance  $d_{\max}$ :

$$p(r_0, d_{\max}, d|N, \hat{d}) \propto \mathcal{L}(N, \hat{d}|d, r_0, d_{\max}) \pi(d|d_{\max}) \pi(r_0) \pi(d_{\max}). \quad (18)$$

Marginalizing over  $d$ , we obtain

$$p(r_0, d_{\max}|N, \hat{d}) \propto \left( \lambda e^{-\lambda} \right) \left[ \frac{3\hat{d}^2}{d_{\max}^3} \Theta(d_{\max} - \hat{d}) \right] \pi(r_0) \pi(d_{\max}). \quad (19)$$

Marginalizing over  $d_{\max}$  lead to a posterior on  $r_0$ . We assume a log-uniform prior for  $r_0$  and a uniform prior for  $d_{\max}$ . Comparing a log-uniform prior with uniform prior, our choice of priors is conservative as it put more a priori weights on lower  $r_0$  and larger  $d_{\max}$ . The prior range for  $r_0$  and  $d_{\max}$  is from 0 to infinity and from  $\hat{d}$  to infinity.

We convert the posterior on  $r_0$  to a posterior on  $A_{\text{yr}}$  using Equation (6) by setting  $L_{-4/3} = 0.63$  and  $\langle M_c^{5/3} \rangle = \bar{M}_c^{5/3}$ . Here  $\bar{M}_c$  is the measured chirp mass for the SMBBH system in question; such a treatment justifies the assumption in Equation (6) that the mass distribution is independent of redshift. As already mentioned,  $L_{-4/3}$  is insensitive to the merger rate evolution within  $z \leq 2$ ; the associated uncertainty is  $\approx 50\%$ , which is much smaller than the Poissonian uncertainty of the merger rate.

We apply the framework developed here to some well-established individual SMBBH candidates with reported estimates of masses, orbital period and eccentricity. Table 1 lists key parameters of these candidates and median values of  $r_0$  and  $A_{\text{yr}}$ . Note that all five binary candidates considered here are in the PTA band, i.e., with  $\mathcal{O}(10)$ -yr periods or sub-pc orbital separations. SMBBH candidates with much longer periods contribute negligibly to the conservative merger rate estimates derived here ( $r_0 \propto T_c^{-1} \propto P_b^{-8/3}$ ).

In Figure 2 we plot the inferred  $r_0$  as a function of chirp mass. There are a couple of features worthy of remark. First, it is apparent that the derived merger rate for 3C 66B is four orders of magnitude above that of OJ 287 or NGC 5548, with both having similar chirp masses. The reason that 3C 66B produces such a high merger rate is due to its very short merger time. If it is a true binary, it is expected to merge in only 500 years, whereas others will typically merge in  $\gtrsim 1$  Myr. OJ 287 is an exception to the previous sentence: if it is real, it will merge in  $10^4$  years. However, it is also much further away than 3C66B, which prevents the merger rate from being as high. The high rate implied by 3C 66B cannot be explained by the uncertainty in mass estimates. Reducing the chirp mass by a factor of two, the typical uncertainty claimed in Iguchi et al. (2010), would only decrease merger rate by a factor of  $2^{5/3} = 3.2$ . Furthermore, if 3C 66B is a

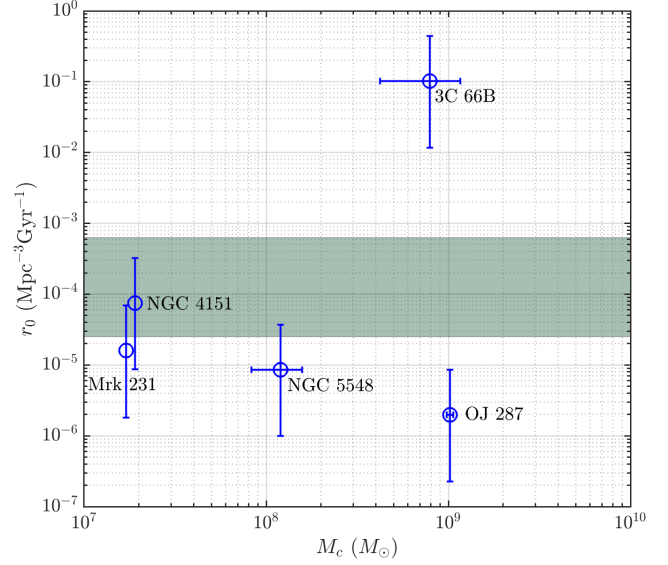


**Figure 2.** The local SMBBH merger rate density  $r_0$  as a function of the binary chirp mass ( $M_c$ ) inferred from several binary candidates; Blue circles mark median values and error bars indicate 68% confidence intervals (see Table 1 for details). The shaded horizontal band corresponds to estimates of galaxy merger rate presented in Conselice (2014).

true SMBBH system, the implied GWB amplitude is nearly two orders of magnitude above the current PTA upper limit  $A_{\text{yr}} \leq 1 \times 10^{-15}$  (see Table 1). In Section 4.1, we use the PTA limit to rule out parameter space in  $(m_1, m_2)$  for 3C 66B.

Second,  $r_0$  inferred from the other four systems are consistent with current estimates of galaxy merger rate density  $r_g$ , which is shown as a shaded horizontal band in Figure 2. For the purpose of illustration, the lower edge of this band corresponds to the lowest estimate ( $r_g \sim 2.5 \times 10^{-5} \text{ Mpc}^{-3} \text{ Gyr}^{-1}$ ) presented in Conselice (2014) for galaxy stellar mass above  $10^{11} M_\odot$  within  $z \leq 1$ , and the upper edge corresponds to the highest estimate ( $r_g \sim 6.3 \times 10^{-4} \text{ Mpc}^{-3} \text{ Gyr}^{-1}$ ) for galaxy stellar mass above  $10^{10} M_\odot$  within  $z \leq 1$ ; see bottom panels of fig. 13 therein.

In the following two subsections, we discuss two special candidates: 3C 66B and OJ 287.

#### 4.1 3C 66B

The elliptical galaxy 3C 66B is located at a redshift of 0.0213. Sudou et al. (2003) observed variations in the radio core position with a period of 1.05 years and interpreted this as due to the orbital motion of an SMBBH. The proposed binary system, with inferred total mass of  $5.4 \times 10^{10} M_\odot$  and mass ratio of 0.1, was subsequently ruled out with 95% confidence by Jenet et al. (2004) using timing observations of PSR B1855+09 presented in Kaspi et al. (1994). Iguchi et al. (2010) performed follow-up observations of the source and obtained significantly lower mass estimates  $-m_1 = 12_{-2}^{+5} \times 10^8 M_\odot$  and  $m_2 = 7.0_{-6.4}^{+4.7} \times 10^8 M_\odot$  assuming a circular orbit. We note that this is below current PTA sensitivities on individual SMBBHs (see, e.g., Zhu et al. 2014).

Following the procedure described above, we compute

Name	$z$	$d_L$ (Mpc)	$m_1$ ( $10^8 M_\odot$ )	$m_2$ ( $10^8 M_\odot$ )	$P_b$ (yr)	$e_0$	Ref.	$M_c$ ( $10^8 M_\odot$ )	$T_c$ (Myr)	$r_0$ ( $\text{Mpc}^{-3} \text{Gyr}^{-1}$ )	$A_{\text{yr}}$ ( $10^{-16}$ )
3C 66B	0.0213	95.7	$12^{+5}_{-2}$	$7.0^{+4.7}_{-6.4}$	1.05	0	(1)	$7.92 \pm 3.7$	$5.1 \times 10^{-4}$	0.1	860
OJ 287	0.3056	1635	$183 \pm 1$	$1.5 \pm 0.1$	12.1	0.7	(2)	$10.23 \pm 0.43$	$1.1 \times 10^{-2}$	$2.0 \times 10^{-6}$	4.7
NGC 5548	0.0172	77.1	$1.51 \pm 0.48$	$1.26 \pm 0.4$	14.1	0.13	(3)	$1.20 \pm 0.37$	11.5	$8.6 \times 10^{-6}$	1.6
NGC 4151	0.0033	14.6	0.44	0.12	15.9	0.42	(4)	0.19	183.5	$7.5 \times 10^{-5}$	1.1
Mrk 231	0.0422	153	1.46	0.04	1.2	0	(5)	0.17	0.43	$1.6 \times 10^{-5}$	0.4

**Table 1.** Parameters of SMBBH candidates, including redshift ( $z$ ), luminosity distance ( $d_L$ ), black hole masses ( $m_1$  and  $m_2$ ), the observed binary orbital period ( $P_b$ ) and eccentricity ( $e_0$ ). Note that  $e_0 = 0$  was assumed for 3C 66B and Mrk 231 in the original publications. Mass errors for NGC 4151 and Mrk 231 are either unavailable or difficult to interpret and thus ignored. References: (1). [Iguchi et al. \(2010\)](#), (2). [Valtonen et al. \(2016\)](#), (3). [Li et al. \(2016\)](#), (4). [Bon et al. \(2012\)](#), (5). [Yan et al. \(2015\)](#). We also derive the binary chirp mass ( $M_c$ ), the coalescence time  $T_c$  and the median estimates of the SMBBH merger rate  $r_0$  and the GWB signal amplitude  $A_{\text{yr}}$ .

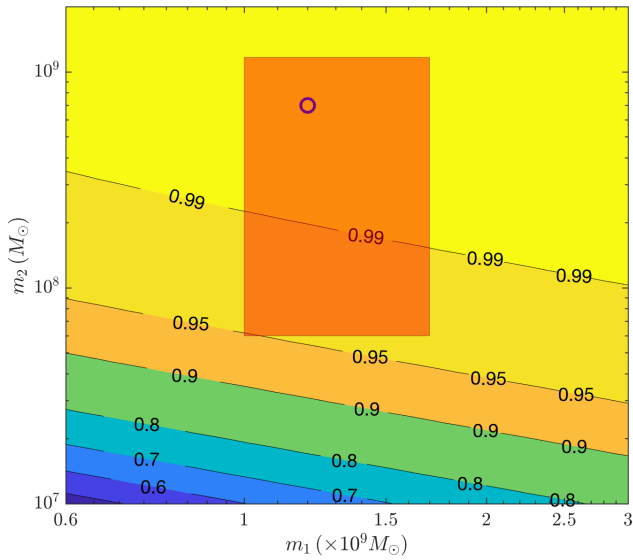


**Figure 3.** The probability  $p(A_{\text{yr}} > 10^{-15})$  if 3C 66B is a true SMBBH system. The red shaded box encompasses the (presumably) 68% confidence intervals reported in [Iguchi et al. \(2010\)](#).

the probability distribution of the GWB signal amplitude  $A_{\text{yr}}$  if we take 3C 66B as a true SMBBH system. We fix the orbital period at 1.05 years; Given its small uncertainty of 0.03 years, our results are not significantly affected by such a simplification. Figure 3 shows the probability that  $A_{\text{yr}} > 10^{-15}$  for a range of masses<sup>3</sup>. The red shaded box encompasses the (presumably 68% confidence) error region reported in [Iguchi et al. \(2010\)](#), whereas the blue circle marks the median estimate. One can see that the median masses can already be ruled out by current PTA upper limits with more than 99% confidence, whereas the entire error box is in tension with PTA observations with 95% probability. This implies that 3C 66B is unlikely to contain an SMBBH.

<sup>3</sup> Note that stronger statements can be made if the full posterior of  $A_{\text{yr}}$  from PTAs is used to perform the consistency test between a model and the data ([Shannon et al. 2015](#)).

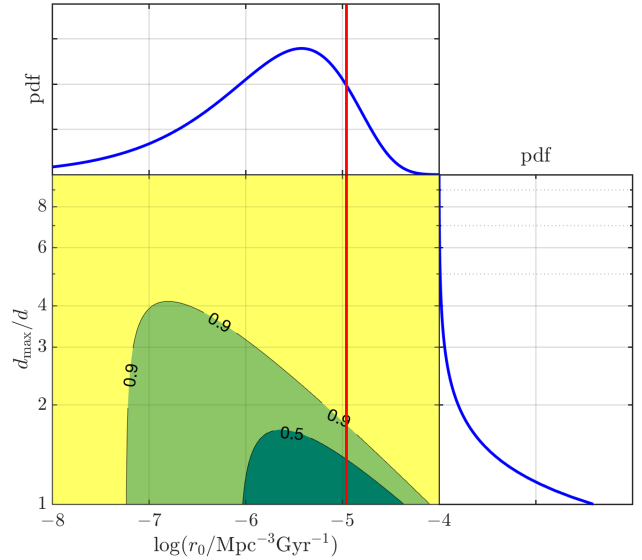


**Figure 4.** The posterior probability density on the merger rate density  $r_0$  of OJ 287-like SMBBHs and the horizon distance  $d_{\text{max}}$ . The red vertical line marks the naive rate estimator  $\hat{r}_0$  given in Equation (12). The contour lines mark the confidence regions.

## 4.2 OJ 287

OJ 287 is a BL Lac object with 12-year quasi-periodic variations in optical light curves. Its observations dated back to 1890s and it was proposed as an SMBBH candidate first by [Sillanpaa et al. \(1988\)](#) with later refinement by [Valtonen et al. \(2008\)](#). Here the model is that a secondary black hole is in an eccentric orbit around a primary black hole, crossing the accretion disk of the primary once every 12 years. This binary system is described with the following parameters:  $(m_1, m_2) = (1.83 \times 10^{10}, 1.5 \times 10^8) M_\odot$ , orbital eccentricity  $e = 0.7$ , observed orbital period  $P_b = 12.07$  yr and redshift  $z = 0.3056$  ([Valtonen et al. 2016](#)), leading to a short merger time  $T_c = 1.6 \times 10^4$  yr. The spin of the primary black hole is ignored as its effect on the GWB at low frequencies is negligible ([Zhu et al. 2011](#)).

We compute probability distribution  $p(A_{\text{yr}})$  under the assumption that OJ 287 is a true SMBBH system. First, the naive estimator of merger rate given by Equation (12) is  $1.1 \times 10^{-5} \text{Mpc}^{-3} \text{Gyr}^{-1}$ . Figure 4 shows the posterior probability of the merger rate density  $r_0$  and  $d_{\text{max}}$ . The red vertical line

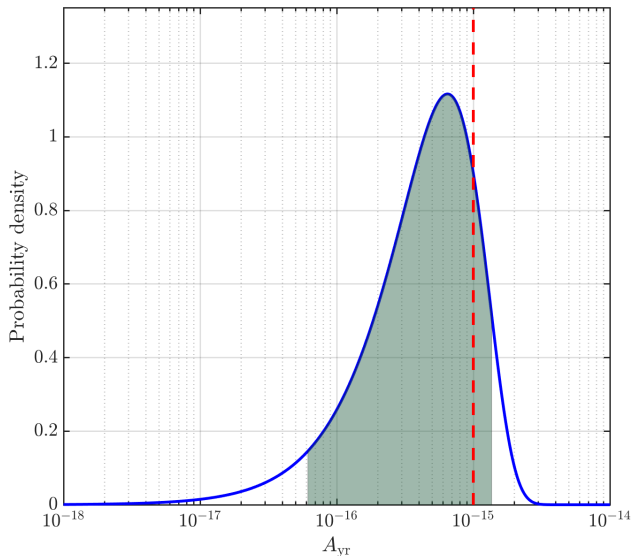


**Figure 5.** The probability distribution of the GWB amplitude  $A_{\text{yr}}$  under the assumption that OJ 287 is a true SMBBH system. The red vertical line marks the PTA upper limit of  $10^{-15}$ . The shaded region corresponds to 90% confidence interval.

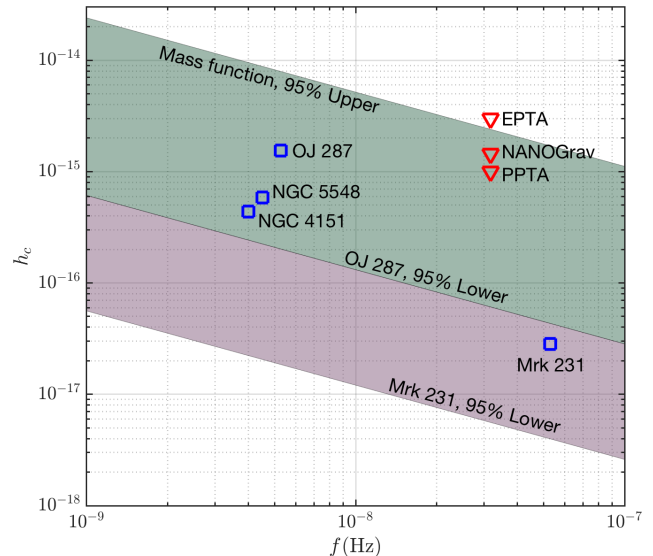
marks the naive estimator  $\hat{r}_0$ . After marginalizing over the unknown  $d_{\text{max}}$ , we find the merger rate density of OJ 287-like SMBBHs to be in  $(2.3 \times 10^{-7}, 8.5 \times 10^{-6}) \text{ Mpc}^{-3} \text{ Gyr}^{-1}$  with 68% confidence.

Figure 5 shows the probability distribution of the GWB amplitude  $A_{\text{yr}}$  transformed from the marginalized posterior distribution of merger rate. We find that 1)  $A_{\text{yr}}$  lies between  $1.6 \times 10^{-16}$  and  $9.7 \times 10^{-16}$  with 68% confidence and 2)  $A_{\text{yr}} > 6.1 \times 10^{-17}$  with 95% confidence.

## 5 SUMMARY AND DISCUSSIONS

We summarize our main results in Figure 6. The shaded regions are determined by the minimum and maximum amplitudes derived in this work. The maximum is the 95% confidence upper limit  $A_{\text{yr}} \leq 2.4 \times 10^{-15}$ , if we consider five models of black hole mass function to be equally likely in Section 3. The minimum is the 95% confidence lower limit  $A_{\text{yr}} \geq 6.1 \times 10^{-17}$  if OJ 287 is a true SMBBH system. If at least one of OJ 287, NGC 5548, NGC 4151 and Mrk 231 host a true SMBBH with parameters inferred in the literature,  $A_{\text{yr}} \geq 5.6 \times 10^{-18}$  with 95% confidence. Red triangles mark the 95% confidence upper limits from three PTA experiments<sup>4</sup>:  $1 \times 10^{-15}$  from PPTA (Shannon et al. 2015),  $1.45 \times 10^{-15}$  from NANOGrav (Arzoumanian et al. 2018) and  $3 \times 10^{-15}$  from EPTA (Lentati et al. 2015).

Our calculations of the maximum amplitude provide a straightforward interpretation of PTA upper limits – if the



**Figure 6.** Characteristic amplitude ( $h_c$ ) of the GWB signal from SMBBHs. The shaded bands are determined by the minimum and maximum amplitudes (all at 95% confidence level) derived in this work. Red triangles are 95% confidence upper limits from various PTA experiments. Blue squares are the median estimates of  $A_{\text{yr}}$  listed in Table 1 extrapolated to twice the observed orbital frequency for several SMBBH candidates.

GWB signal was stronger, we would have been able to see more single black holes left over from SMBBH merger events. We conclude that existing PTA limits constrain only the extremely optimistic models, in agreement with the recent work by Middleton et al. (2018).

While current PTAs steadily increase their sensitivities and next-generation PTAs are being commissioned or planned for new telescopes such as FAST (Nan et al. 2011), MeerKAT (Bailes et al. 2018) and ultimately the SKA, it is critical to understand what is the minimum level of GWB from the cosmic population of SMBBHs.

We presented in this paper a novel Bayesian framework to estimate the minimum amplitude of this highly-sought signal. We demonstrated that a single gold-plated detection of an SMBBH system in the local Universe immediately implies a lower limit on the GWB. We applied our framework to several well-established sub-parsec SMBBH candidates. We found that 3C 66B is unlikely to host an SMBBH system because if it was, it would 1) suggest a GWB signal that is inconsistent with existing upper limits at high ( $> 99\%$ ) confidence and 2) indicate an SMBBH merger rate that is three orders of magnitude higher than current estimates of galaxy merger rate.

If OJ 287 is a true SMBBH system with parameters suggested in Valtonen et al. (2016), a median GWB is to have  $A_{\text{yr}} = 4.7 \times 10^{-16}$ . While this may sound like a good news for PTAs, we note, however, that a lower total mass of  $4 \times 10^8 M_{\odot}$  was derived in Liu & Wu (2002) and further supported recently by Britzen et al. (2017), in contrast to  $1.8 \times 10^{10} M_{\odot}$  used in our calculations. This would reduce the  $A_{\text{yr}}$  estimate by a factor of 600 (since  $A_{\text{yr}} \propto M_c^{5/3}$ ) if other parameters remain unchanged.

<sup>4</sup> Note that such PTA upper limits were set for a  $-2/3$  power-law GWB rather than at a single frequency of  $1 \text{ yr}^{-1}$ . In fact, because of the steep spectrum of the GWB signal, PTA experiments are most sensitive to a much lower frequency. This frequency is comparable to  $1/T_{\text{obs}}$  with  $T_{\text{obs}} \gtrsim 10$  yrs being the data span.

Blue squares in Figure 6 show the median predictions of the GWB amplitude at twice the orbital frequency for several SMBBH candidates. These sources are all in the GW dominant regime. Apart from being interesting targets for continuous GW searches, they collectively suggest a sizeable GWB signal for PTAs. Without looking into specific details of each source for which no quantified statistical significance is available, a simple argument is that  $A_{\text{yr}} > 5.6 \times 10^{-18}$  at 95% confidence if at least one of these candidates is a true binary black hole with parameters inferred in the literature.

We suggest that advances in the following areas will be helpful to improve our predictions. First, quantified statistical significance of the SMBBH candidates can be built into our framework to produce more robust GWB predictions. Second, better understanding of the discovery efficiency, sensitive volume and survey completeness of various observational campaigns that search for sub-parsec SMBBHs will lead to tighter constraints on the SMBBH merger rate and the GWB amplitude.

Finally, our calculations focused on the  $h_c \sim f^{-2/3}$  power spectrum. The actual signal spectral shape is likely to deviate from this. First, the small number of binaries contributing to the background reduces signal power at  $f \gtrsim 1 \text{ yr}^{-1}$  (Sesana et al. 2008; Ravi et al. 2012). Second, effects of binary eccentricity (Enoki & Nagashima 2007; Huerta et al. 2015) and the interaction between SMBBHs and their environments (Sesana et al. 2004; Ravi et al. 2014) are known to attenuate the signal power at  $f \lesssim 0.1 \text{ yr}^{-1}$  (see Kelley et al. 2017, for details). Nevertheless, the method presented here<sup>5</sup> is especially useful for obtaining leading-order predictions for the GWB signal. In particular, when a new SMBBH candidate is discovered, our method allows quick evaluation of its implications for the GWB, and potentially enable constraints to be placed on black hole masses. In short, an *unambiguous* SMBBH detection will have immediate implications to PTAs.

## ACKNOWLEDGEMENTS

We thank the referee for very useful comments. We also thank Alberto Sesana, Yuri Levin, Wang Jian-Min, Li Yan-Rong and Lu Youjun for insightful discussions. X.Z. & E.T. are supported by ARC CE170100004. E.T. is supported through ARC FT150100281. W.C. is supported by the *Ministerio de Economía y Competitividad* and the *Fondo Europeo de Desarrollo Regional* (MINECO/FEDER, UE) in Spain through grant AYA2015-63810-P.

## REFERENCES

Aasi J., et al., 2015, *Classical and Quantum Gravity*, **32**, 074001  
 Abbott B. P., et al., 2016a, *Physical Review X*, **6**, 041015  
 Abbott B. P., et al., 2016b, *Physical Review Letters*, **116**, 061102  
 Abbott B. P., et al., 2016c, *Physical Review Letters*, **116**, 131102  
 Abbott B. P., et al., 2017a, *Physical Review Letters*, **119**, 161101  
 Abbott B. P., et al., 2017b, *ApJ*, **851**, L35  
 Abbott B. P., et al., 2018, *Physical Review Letters*, **120**, 091101

Acernese F., et al., 2015, *Classical and Quantum Gravity*, **32**, 024001  
 Arzoumanian Z., et al., 2018, *ApJ*, **859**, 47  
 Bailes M., et al., 2018, preprint, ([arXiv:1803.07424](https://arxiv.org/abs/1803.07424))  
 Begelman M. C., Blandford R. D., Rees M. J., 1980, *Nature*, **287**, 307  
 Bon E., et al., 2012, *ApJ*, **759**, 118  
 Bonetti M., Sesana A., Barausse E., Haardt F., 2018, *MNRAS*, **477**, 2599  
 Britzen S., et al., 2017, in *Journal of Physics Conference Series*. p. 012005, doi:10.1088/1742-6596/942/1/012005  
 Conselice C. J., 2014, *ARA&A*, **52**, 291  
 D’Orazio D. J., Haiman Z., Schiminovich D., 2015, *Nature*, **525**, 351  
 Demorest P. B., et al., 2013, *ApJ*, **762**, 94  
 Detweiler S., 1979, *ApJ*, **234**, 1100  
 Dvorkin I., Barausse E., 2017, *MNRAS*, **470**, 4547  
 Enoki M., Nagashima M., 2007, *Progress of Theoretical Physics*, **117**, 241  
 Flanagan É. É., Hughes S. A., 1998, *Phys. Rev. D*, **57**, 4535  
 Foster R. S., Backer D. C., 1990, *ApJ*, **361**, 300  
 Hellings R. W., Downs G. S., 1983, *ApJ*, **265**, L39  
 Hobbs G., et al., 2010, *Class. Quant. Grav.*, **27**, 084013  
 Huerta E. A., McWilliams S. T., Gair J. R., Taylor S. R., 2015, *Phys. Rev. D*, **92**, 063010  
 Iguchi S., Okuda T., Sudou H., 2010, *ApJ*, **724**, L166  
 Jaffe A. H., Backer D. C., 2003, *ApJ*, **583**, 616  
 Jenet F. A., Lommen A., Larson S. L., Wen L., 2004, *ApJ*, **606**, 799  
 Jenet F. A., Hobbs G. B., Lee K. J., Manchester R. N., 2005, *ApJ*, **625**, L123  
 Jenet F. A., Hobbs G. B., van Straten W., et al. 2006, *ApJ*, **653**, 1571  
 Kaspi V. M., Taylor J. H., Ryba M. F., 1994, *ApJ*, **428**, 713  
 Kelley L. Z., Blecha L., Hernquist L., Sesana A., Taylor S. R., 2017, *MNRAS*, **471**, 4508  
 Kramer M., Champion D. J., 2013, *Class. Quant. Grav.*, **30**, 224009  
 Kulier A., Ostriker J. P., Natarajan P., Lackner C. N., Cen R., 2015, *ApJ*, **799**, 178  
 Lazio T. J. W., 2013, *Class. Quant. Grav.*, **30**, 224011  
 Lentati L., et al., 2015, *MNRAS*, **453**, 2576  
 Li Y.-R., Ho L. C., Wang J.-M., 2011, *ApJ*, **742**, 33  
 Li Y.-R., et al., 2016, *ApJ*, **822**, 4  
 Liu F. K., Wu X.-B., 2002, *A&A*, **388**, L48  
 Maggiore M., 2000, *Physics Reports*, **331**, 283  
 Manchester R. N., 2013, *Class. Quant. Grav.*, **30**, 224010  
 Manchester R. N., et al., 2013, *Publ. Astron. Soc. Australia*, **30**, 17  
 Marconi A., Risaliti G., Gilli R., Hunt L. K., Maiolino R., Salvati M., 2004, *MNRAS*, **351**, 169  
 McConnell N. J., Ma C.-P., 2013, *ApJ*, **764**, 184  
 McLaughlin M. A., 2013, *Class. Quant. Grav.*, **30**, 224008  
 McWilliams S. T., Ostriker J. P., Pretorius F., 2014, *ApJ*, **789**, 156  
 Middleton H., Chen S., Del Pozzo W., Sesana A., Vecchio A., 2018, *Nature Communications*, **9**, 573  
 Mutlu-Pakdil B., Seigar M. S., Davis B. L., 2016, *ApJ*, **830**, 117  
 Nan R., et al., 2011, *International Journal of Modern Physics D*, **20**, 989  
 Phinney E. S., 2001, preprint, ([arXiv:astro-ph/0108028](https://arxiv.org/abs/astro-ph/0108028))  
 Planck Collaboration et al., 2016, *A&A*, **594**, A13  
 Quinlan G. D., 1996, *New Astronomy*, **1**, 35  
 Rajagopal M., Romani R. W., 1995, *ApJ*, **446**, 543  
 Ravi V., Wyithe J. S. B., Hobbs G., Shannon R. M., Manchester R. N., Yardley D. R. B., Keith M. J., 2012, *ApJ*, **761**, 84  
 Ravi V., Wyithe J. S. B., Shannon R. M., Hobbs G., Manchester R. N., 2014, *MNRAS*, **442**, 56

<sup>5</sup> Our codes are publicly available at [https://github.com/ZhuXJ1/PTA\\_GWBminmax](https://github.com/ZhuXJ1/PTA_GWBminmax)

Ryu T., Perna R., Haiman Z., Ostriker J. P., Stone N. C., 2018, *MNRAS*, **473**, 3410

Sazhin M. V., 1978, *Soviet Astronomy*, **22**, 36

Sesana A., 2013, *MNRAS*, **433**, L1

Sesana A., Haardt F., Madau P., Volonteri M., 2004, *ApJ*, **611**, 623

Sesana A., Vecchio A., Colacino C. N., 2008, *MNRAS*, **390**, 192

Sesana A., Shankar F., Bernardi M., Sheth R. K., 2016, *MNRAS*, **463**, L6

Shankar F., 2013, *Classical and Quantum Gravity*, **30**, 244001

Shankar F., Weinberg D. H., Miralda-Escudé J., 2009, *ApJ*, **690**, 20

Shannon R. M., Ravi V., Lentati L. T., et al., 2015, *Science*, **349**, 1522

Sillanpaa A., Haarala S., Valtonen M. J., Sundelius B., Byrd G. G., 1988, *ApJ*, **325**, 628

Sudou H., Iguchi S., Murata Y., Taniguchi Y., 2003, *Science*, **300**, 1263

Taylor S. R., Vallisneri M., Ellis J. A., Mingarelli C. M. F., Lazio T. J. W., van Haasteren R., 2016, *ApJ*, **819**, L6

Thorne K. S., 1987, in Hawking S., Israel W., eds, *Three Hundred Years of Gravitation*. Cambridge Uni. Press, Cambridge

Ueda Y., Akiyama M., Hasinger G., Miyaji T., Watson M. G., 2014, *ApJ*, **786**, 104

Valtonen M. J., et al., 2008, *Nature*, **452**, 851

Valtonen M. J., et al., 2016, *ApJ*, **819**, L37

Verbiest J. P. W., et al., 2016, *Mon. Not. R. Astron. Soc.*, **458**, 1267

Wyithe J. S. B., Loeb A., 2003, *ApJ*, **590**, 691

Yan C.-S., Lu Y., Dai X., Yu Q., 2015, *ApJ*, **809**, 117

Yardley D. R. B., et al., 2011, *MNRAS*, **414**, 1777

Yu Q., Lu Y., 2008, *ApJ*, **689**, 732

Zhu X.-J., Howell E., Regimbau T., Blair D., Zhu Z.-H., 2011, *ApJ*, **739**, 86

Zhu X.-J., Howell E. J., Blair D. G., Zhu Z.-H., 2013, *MNRAS*, **431**, 882

Zhu X.-J., et al., 2014, *MNRAS*, **444**, 3709

van Haasteren R., Levin Y., Janssen G. H., et al. 2011, *MNRAS*, **414**, 3117

## APPENDIX A: THE LOCAL BLACK HOLE MASS FUNCTION

Black hole masses ( $M_{BH}$ ) are normally estimated from the black hole-host galaxy scaling relations. A comparison among the local black hole mass functions based on different scaling relations can be found in, for example, fig. 1 of Yu & Lu (2008) and fig. 5 of Shankar et al. (2009). In this work, we consider five models that are derived using different methods. They are visually represented in Fig. A1 and we provide brief descriptions below.

Marconi et al. (2004) adopted both the  $M_{BH} - \sigma$  and the  $M_{BH} - L_{Bulge}$  relations and found similar results. Here we use their model from all types of galaxies. The model of Li et al. (2011) is obtained using the galaxy catalogue of the UKIDSS Ultra Deep Survey combined with the empirical correlation between  $M_{BH}$  and spheroid mass (the  $M_{BH} - M_{sph}$  relation). We also include the mass function from Shankar (2013) and take the model that assumes all local galaxies follow the early-type  $M_{bh} - \sigma$  relation of McConnell & Ma (2013). This model is suggested to be an *upper limit* to the local mass function.

Recently, Mutlu-Pakdil et al. (2016) estimated black hole masses with the  $M_{BH} - P$  relation (with  $P$  being the

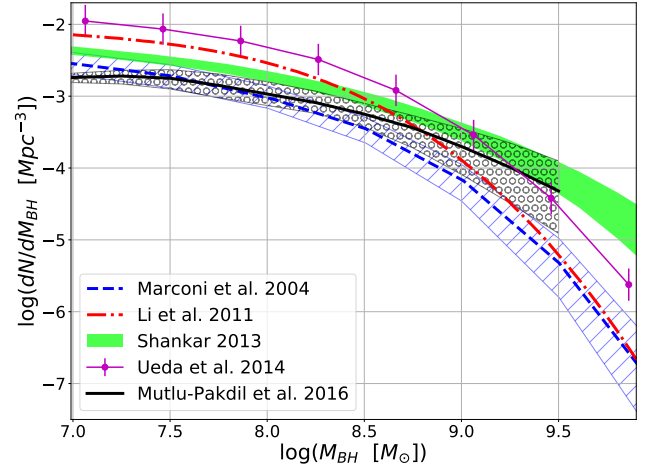


**Figure A1.** Five models of the local black hole mass function used in Section 3 and for upper bounds on the GWB amplitude illustrated in Figure 1. The  $1-\sigma$  uncertainties are shown as filled regions, shaded areas or error bars. As no uncertainty was provided in the model of Li et al. (2011), we assume 20% variation for  $\log(dN/dM_{BH})$ .

**Table A1.** The number density ( $N_0$ ) and mass density ( $M_0$ ) of supermassive black holes for mass functions shown in Figure A1.

Model	$N_0$ [ $10^{-3} \text{Mpc}^{-3}$ ]	$M_0$ [ $10^5 M_\odot \text{Mpc}^{-3}$ ]
Marconi et al. (2004)	2.33	1.86
Li et al. (2011)	6.35	4.70
Shankar (2013)	4.17	6.01
Ueda et al. (2014)	10.56	9.48
Mutlu-Pakdil et al. (2016)	2.29	3.18

galactic spiral arm pitch angle) for late-type galaxies and the  $M_{BH} - n$  relation (with  $n$  being the Sersic index) for early-type galaxies. This model gives the lowest value at the lower mass end. The four models mentioned so far are all based on optical observations. We further consider the model by Ueda et al. (2014) in which the mass function was derived from the X-ray luminosity function of active galactic nuclei. In this case, the X-ray luminosity can be related to the mass accretion rate onto black holes; the mass function can then be derived through the continuity equation.

As one can see from Fig. A1, the five models are broadly consistent with each other. Overall, the uncertain range is about an order of magnitude between  $10^7$  and  $10^9 M_\odot$  and larger at the higher mass end. We integrate these mass functions from  $10^7$  up to  $10^{10} M_\odot$  to compute the number density  $N_0$  and the mass density  $M_0$ :

$$N_0 = \int_{10^7 M_\odot} \Phi(M) dM, \quad M_0 = \int_{10^7 M_\odot} M \Phi(M) dM. \quad (\text{A1})$$

Here  $\Phi(m) = dN/dM$  is the black hole mass function. The results are presented in Table A1.

This paper has been typeset from a  $\text{\LaTeX}$  file prepared by the author.